Warping- and inversion-asymmetry-induced cyclotron-harmonic transitions in InSb

M. H. Weiler, R. L. Aggarwal, and B. Lax

Francis Bitter National Magnet Laboratory and Department of Physics, Massachusetts Institute of Technology, Cambridge, Massachusetts 02139

(Received 10 January 1977)

Selection rules are obtained for harmonics of the cyclotron resonance transition in InSb, such as $2\omega_c$ ($\Delta n = 2$, $\Delta m_s = 0$), $3\omega_c$ ($\Delta n = 3$, $\Delta m_s = 0$), etc., and spin-shifted harmonics such as $2\omega_c + \omega_s$ ($\Delta n = 2$, $\Delta m_s = -1$), etc., where Δn and Δm_s are the changes in the Landau quantum number and the z component of the spin angular momentum. These transitions are induced by warping and inversion-asymmetry effects. The complete $\vec{k}\cdot\vec{p}$ Hamiltonian is obtained to second order in $\vec{k}$ and to first order in the applied magnetic field $\vec{H}$ for the coupled conduction band (Γ_6), light- and heavy-hole valence bands (Γ_8) and split-off valence band (Γ_7). This Hamiltonian treats the interactions with higher bands as second-order perturbations, and includes terms proportional to three new parameters which arise from the spin-orbit splitting of these higher bands. A group-theoretical analysis is carried out for $\vec{H}$ in the $(1\bar{1}0)$ plane including $k_H \neq 0$, k_H being the momentum component along the direction of the applied magnetic field. The selection rules for the intra-conduction-band transition $2\omega_c$, $2\omega_c + \omega_s$, and $3\omega_c$ are in agreement with experiment but with one important exception: that a strong $2\omega_c$ transition observed for $\vec{H} \| [001]$ in the polarization $\vec{E} \perp \vec{H}$ is not predicted by the above group-theoretical analysis.

I. INTRODUCTION

As the result of many magneto-optical investigations and theoretical calculations, most properties of the conduction and valence bands in InSb are reasonably well understood. An important exception has been a number of observations in n-type InSb of the second and third harmonics of cyclotron resonance, denoted by $2\omega_c$ and $3\omega_c$,[1-5] as well as the spin-shifted harmonic denoted by $2\omega_c + \omega_s$.[4] These transitions have been observed along with the allowed combined resonance $\omega_c + \omega_s$ transition,[6] and the LO-phonon-assisted resonances $\omega_c + \omega_{LO}$, $2\omega_c + \omega_{LO}$, etc.[1,2] The latter have been explained by the theoretical work of Enck, Saleh, and Fan[1] and Bass and Levinson.[7] Bell and Rogers obtained selection rules for warping and inversion-asymmetry induced harmonic transitions, for an applied magnetic field $\vec{H}$ parallel to a [001] crystal axis.[8] Favrot, Aggarwal, and Lax[5] recently reported that the intensity of these transitions exhibits marked anisotropy with respect to the crystal orientation relative to the applied magnetic field, in addition to its dependence on the optical polarization. We have obtained the selection rules for cyclotron harmonic transitions induced by warping and inversion asymmetry for the magnetic field applied along the crystal axes [001], [110], and [111].[9] These selection rules are consistent with the experimental results with one important exception. Favrot *et al.*[5] observed a strong $2\omega_c$ absorption for the light polarization vector $\vec{E} \perp \vec{H}$ with $\vec{H} \| [001]$. This is not predicted either by us or by Bell and Rogers,[8] or by the recent work of Zawadzki and Wlasak[10] for this orientation.

In the present work, the selection rules for these intraband transitions are obtained in the spirit of the treatment by Pidgeon and Groves of inversion asymmetry and warping-induced interband transitions.[11] They treated effects of warping and inversion asymmetry (the linear k term) as perturbations in the "quasi-Ge" model of Pidgeon and Brown.[12] In this model the energies of the conduction band, light- and heavy-hole bands and the split-off valence band are calculated in an approximate coupled band scheme, suggested by the work of Luttinger[13] and Roth, Lax, and Zwerdling,[14] which includes nonparabolic and "quantum" effects[15] and a portion of the warping effects, in such a way that only 4×4 matrices had to be diagonalized for each Landau quantum number n and for the a (conduction-electron spin up) and b (conduction-electron spin down) sets. This model was reviewed in detail by Aggarwal.[16]

The InSb energy bands are illustrated in Fig. 1. For the case of zero magnetic field ($H = 0$), the k dependence is given schematically for the bands considered "nearly degenerate" in the quasi-Ge model, labeled with both single and double group notations. In a magnetic field ($H \neq 0$), the coupled Landau levels are illustrated for the a and b sets, labeled with the principal Landau quantum number following the notation of Pidgeon and Brown.[12]

In order to find all allowed transitions among the conduction band states of Fig. 1, we have obtained from the tables of Koster, Dimmock, Wheeler, and Statz (KDWS),[17] all allowed terms

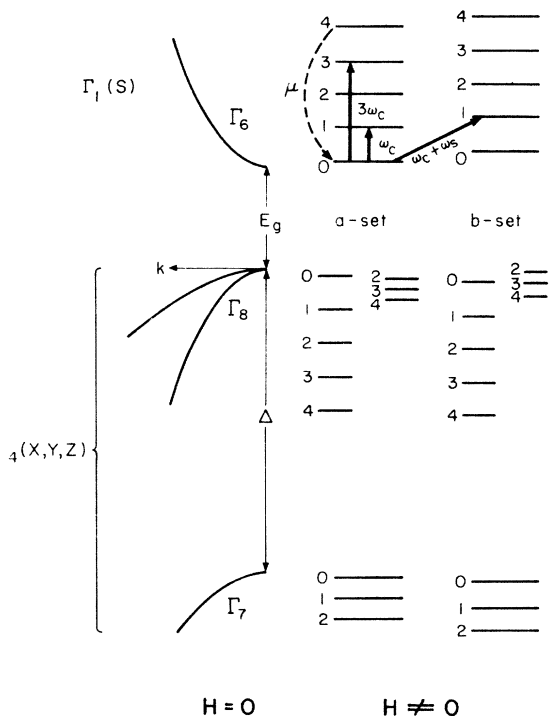

FIG. 1. Schematic representation of the InSb conduction and valence bands at the Γ point, labeled as both single-group (Γ_1 and Γ_4) and double-group (Γ_6, Γ_7, and Γ_8) representations of the T_d group. On the left, the k dependence is illustrated in zero magnetic field ($H=0$). On the right are shown, for $H\neq 0$, the resulting Landau levels and intraconduction-band transitions ω_c, $\omega_c+\omega_s$, and $3\omega_c$. The $3\omega_c$ transition is induced by the coupling between the $n=4$ and $n=0$ Landau levels proportional to the warping parameter μ.

up to second order in $\vec{k}$ and to first order in $\vec{H}$ in the 8×8 matrix Hamiltonian for the $\Gamma_6(J=\frac{1}{2})$ conduction band, the $\Gamma_8(J=\frac{3}{2})$ light- and heavy-hole bands, and the $\Gamma_7(J=\frac{1}{2})$ spin-orbit–split-off valence band. We find, in addition to the parameters described by Luttinger[13] for Ge and by Kane[18] for InSb, three new parameters N_1, N_2, and N_3: N_1 contributes to the conduction band g factor, and N_2 and N_3 have effects similar to the linear-k term and the terms proportional to the Kane parameter G.[18] These new parameters are shown in the Appendix to arise from the spin-orbit splitting of higher bands of Γ_8 symmetry.

In the approximate quasi-Ge model,[12] the allowed intraband optical transitions are, for polarizations $\vec{E}\perp\vec{H}$, $a(n)\rightarrow a(n+1)$, and $b(n)\rightarrow b(n+1)$ corresponding to the cyclotron resonance transition ω_c, and for the $\vec{E}\parallel\vec{H}$ polarization $a(n)\rightarrow b(n+1)$ corresponding to the combined resonance transition $\omega_c+\omega_s$,[1] where ω_s is the spin-flip frequency. The ω_c and $\omega_c+\omega_s$ transitions, which are allowed for all orientations of magnetic field, are included in Fig. 1. It should be pointed out that because of nonparabolicity and quantum effects, the "harmonic" transitions $n\omega_c$ do not occur exactly at the frequency n times ω_c. Therefore the notation $n\omega_c$ is used merely for labeling purposes. Secondly, we show only transitions allowed for $k_H=0$, where k_H is the electron momentum parallel to the applied magnetic field $\vec{H}$.

The main effect of the small terms neglected in the Pidgeon and Brown Hamiltonian is to allow extra weak optical transitions. For $k_H=0$ the warping terms μ and q[13] allow third-harmonic transitions $a(n)\rightarrow a(n+3)$ denoted by $3\omega_c$, as observed for the heavy holes in Ge.[19] The inversion-asymmetry parameters allow the second-harmonic transitions $a(n)\rightarrow a(n+2)$ denoted by $2\omega_c$ and $a(n)\rightarrow b(n+2)$ denoted by $2\omega_c+\omega_s$. The inversion-asymmetry parameters are: the linear-k parameter C,[11] the Kane parameter G,[18] and the new parameters N_2 and N_3. For $k_H\neq 0$ the warping terms also induce second-harmonic transitions,[19] and the inversion-asymmetry terms induce third-harmonic transitions. The optical polarizations in which these extra transitions occur depend on the orientation of the crystal axes relative to the applied magnetic field.

The mechanism for the warping-induced $3\omega_c$ transition is illustrated in Fig. 1. For certain orientations of the crystal relative to the applied magnetic field, a term proportional to the warping parameter μ couples the $a(4)$ level to the $a(0)$ ground state in the conduction band, giving the $a(0)$ level an admixture of the $a(4)$ wave function. Then the optical-transition matrix element connecting $a(4)$ to $a(3)$ for $\vec{E}\perp\vec{H}$ also gives a weaker transition $a(0)\rightarrow a(3)$, denoted by $3\omega_c$, as illustrated.

The strength of these extra transitions, as a function of the six parameters μ, q, C, G, N_2, and N_3, is found by calculating the optical matrix elements among the levels of the quasi-Ge model, including the warping- and inversion-asymmetry perturbations as first-order corrections to the wave functions. In Sec. II below we find the complete InSb $\vec{k}\cdot\vec{p}$ Hamiltonian to first order in $\vec{H}$ and to second order in $\vec{k}$, and in Sec. III describe the quasi-Ge model for the magnetic field $\vec{H}$ in the $(1\bar{1}0)$ crystal plane. In Sec. IV we give the warping- and inversion-asymmetry perturbations, and in Sec. V we calculate the transition matrix elements from these perturbations, and the resulting selection rules for intraband transitions for the magnetic field in the three principal directions [001], [110], and [111]. These selection rules are compared with the experimental results in Sec. VI.

II. InSb HAMILTONIAN TO SECOND ORDER IN $\vec{k}$

In order to obtain the $\vec{k}\cdot\vec{p}$ matrix Hamiltonian in the quasi-Ge model, that is for the set of coupled bands illustrated in Fig. 1, there have been two different approaches based on group-theoretical techniques. In the first approach,[13,20] one finds interband matrix elements $\vec{p}_{\alpha\beta}$ of the $\vec{k}\cdot\vec{p}$ perturbation Hamiltonian $\hbar\vec{k}\cdot\vec{p}_{\alpha\beta}/m$ and also of the spin-orbit Hamiltonian. For the case of InSb, Kane[18] enumerated all possible combinations of these matrix elements to second order in $\vec{k}$ among the single-group basis states transforming as Γ_1 (conduction band S) and Γ_4 (valence bands X, Y, and Z) of the T_d group. The first-order matrix elements $\vec{p}_{\alpha\beta}$ and second-order combinations involving intermediate states belonging to different representations of the T_d single group, were adjustable parameters of the perturbation Hamiltonian. This Hamiltonian was expressed in terms of linear combinations of the functions X, Y, and Z and of the spin-functions $\uparrow$ and $\downarrow$, which diagonalize the spin-orbit interaction. This Hamiltonian involves matrix elements coupling the various basis states including adjustable parameters multiplying functions to second order in $\vec{k}$. A second approach to obtaining this Hamiltonian was made by Luttinger,[13] who used a group-theoretical analysis to find all allowed matrix elements of $\vec{k}$ and $\vec{k}\times\vec{k}$ among the valence-band states transforming as the Γ_8 representation of the double group. His result involved adjustable parameters which were linear combinations of those of Kane,[18] but included an additional parameter q which is nonzero only in the presence of spin-orbit splittings of the intermediate states. Luttinger's results were extended by Roth *et al.*[14] to include the Γ_7 split-off band. Pidgeon and Brown[12] included the Γ_6 conduction band in their analysis, combining the results of Kane[18] and of Roth *et al.*[14]

In this paper we use the second approach to obtain a complete set of parameters for the coupled Γ_6, Γ_7, and Γ_8 bands and find three new parameters in addition to those of Refs. 14 and 18, which have the same origin as Luttinger's parameter q.[13] Our group theoretical treatment makes use of the KDWS tables of coupling coefficients.[17] Although their basis functions are not stated explicitly, we find these by comparing our resulting matrix with those of Refs. 14 and 18. This set of basis functions is given below, in terms of the basis functions used by Kane.[18]

$$
\begin{aligned}
&a \text{ set}\\
&|1\rangle=\psi^6_{1/2,1/2}=S\uparrow\,,\\
&|3\rangle=\psi^8_{3/2,3/2}=-\frac{i}{\sqrt{2}}(X+iY)\uparrow\,,\\
&|5\rangle=\psi^8_{3/2,-1/2}=\frac{i}{\sqrt{6}}[(X-iY)\uparrow+2Z\downarrow]\,,\\
&|7\rangle=\psi^7_{1/2,-1/2}=-\frac{i}{\sqrt{3}}[(X-iY)\uparrow-Z\downarrow]\,,\\
&b \text{ set}\\
&|2\rangle=\psi^6_{1/2,-1/2}=S\downarrow\,,\\
&|6\rangle=\psi^8_{3/2,1/2}=-\frac{i}{\sqrt{6}}[(X+iY)\downarrow-2Z\uparrow]\,,\\
&|4\rangle=\psi^8_{3/2,-3/2}=\frac{i}{\sqrt{2}}(X-iY)\downarrow\,,\\
&|8\rangle=\psi^7_{1/2,1/2}=-\frac{i}{\sqrt{3}}[(X+iY)\downarrow+Z\uparrow]\,.
\end{aligned}
\tag{1}
$$

The states $|3\rangle$, $|4\rangle$, $|5\rangle$, and $|6\rangle$ are the same, except for an overall factor of $(-i)$, as those used by Pidgeon and Groves.[11] These four states form a representation of the $J=\frac{3}{2}$ (Γ_8) valence band, and, as stated by Pidgeon and Groves, the 4×4 $\vec{k}\cdot\vec{p}$ matrices involving these states agree with those given by Luttinger.[13] The valence-band states are equal to those of Eqs. (23) and (A3) of Roth, Lax, and Zwerdling[14] except for an overall factor of $(-i)$ and an additional factor of (-1) in states $|4\rangle$ and $|6\rangle$, so that our a-set matrices for the valence-band (states $|3\rangle$, $|5\rangle$, and $|7\rangle$)

TABLE I. Parameters of the $\vec{k}\cdot\vec{p}$ Hamiltonian among the InSb Γ_6, Γ_7, and Γ_8 band-edge states.

$f(\vec{k})$	k_x,k_y,k_z	k^2	$(2k_z^2-k_x^2-k_y^2),\sqrt{3}\,(k_x^2-k_y^2)$	$\{k_y,k_z\},\{k_x,k_z\},\{k_x,k_y\}$	$i[k_y,k_z],i[k_z,k_x],i[k_x,k_y]$
$\langle\Gamma_6\|f(\vec{k})\|\Gamma_6\rangle$		F			N_1
$\langle\Gamma_8\|f(\vec{k})\|\Gamma_8\rangle$	C	γ_1	γ_2	γ_3	κ,q
$\langle\Gamma_7\|f(\vec{k})\|\Gamma_7\rangle$		γ_1'			κ'
$\langle\Gamma_6\|f(\vec{k})\|\Gamma_8\rangle$	P		N_2	G	N_3
$\langle\Gamma_6\|f(\vec{k})\|\Gamma_7\rangle$	P'			G'	
$\langle\Gamma_7\|f(\vec{k})\|\Gamma_8\rangle$	C'		γ_2'	γ_3'	κ''

TABLE II. $\vec{k}\cdot\vec{p}$ Hamiltonian matrix $\mathcal{H}$ for InSb band-edge states. The basis states and terms used are defined in Eqs. (1) and (2). The upper triangle is the Hermitian conjugate of the lower triangle.

$\langle 1\vert$	$\langle 3\vert$	$\langle 5\vert$	$\langle 7\vert$	$\langle 2\vert$	$\langle 6\vert$	$\langle 4\vert$	$\langle 8\vert$
$E_g+(F+\frac{1}{2})k^2$ $+(N_1+\frac{1}{2})H_z$							
$\frac{1}{\sqrt{2}}Pk^-+\frac{1}{\sqrt{2}}GF_4^+$ $+\frac{1}{2}N_3H^+$	$-\frac{1}{2}\gamma_1k^2+\frac{1}{2}\gamma_2F_3^1$ $-\frac{3}{2}(\kappa+\frac{9}{4}q)H_z$						
$-\frac{1}{\sqrt{6}}Pk^++\frac{1}{\sqrt{6}}GF_4^-$ $+\frac{1}{2}\sqrt{3}N_3H^-$	$\frac{1}{2}\gamma_2F_3^2+i\frac{1}{2}\sqrt{3}\,\gamma_3F_4^z$ $+Ck_z$	$-\frac{1}{2}\gamma_1k^2-\frac{1}{2}\gamma_2F_3^1$ $+\frac{1}{2}(\kappa+\frac{1}{4}q)H_z$					
$\frac{1}{\sqrt{3}}P'k^+-\frac{1}{\sqrt{3}}G'F_4^-$	$-\frac{1}{\sqrt{2}}\gamma_2'F_3^2-i\frac{1}{2}\sqrt{6}\,\gamma_3'F_4^z$ $+\frac{1}{\sqrt{2}}C'k_z$	$-\frac{1}{\sqrt{2}}\gamma_2'F_3^1$ $-\frac{1}{\sqrt{2}}(\kappa''+1)H_z$	$-\Delta-\frac{1}{2}\gamma_1'k^2$ $+(\kappa'+\frac{1}{2})H_z$				
$(N_1+\frac{1}{2})H^+$	$N_2F_3^1+N_3H_z$	$-\sqrt{\frac{2}{3}}Pk_z+i\sqrt{\frac{2}{3}}GF_4^z$ $-N_2F_3^2$	$-\frac{1}{\sqrt{3}}P'k_z+\frac{i}{\sqrt{3}}G'F_4^z$	$E_g+(F+\frac{1}{2})k^2$ $-(N_1+\frac{1}{2})H_z$			
$-\sqrt{\frac{2}{3}}Pk_z-i\sqrt{\frac{2}{3}}GF_4^z$ $+N_2F_3^2$	$\frac{1}{2}\sqrt{3}\,\gamma_3F_4^+-\frac{1}{2}Ck^-$ $-\frac{1}{2}\sqrt{3}(\kappa+\frac{7}{4}q)H^+$	$\frac{1}{2}\sqrt{3}Ck^+$ $-(\kappa+\frac{5}{2}q)H^-$	$\frac{3}{\sqrt{8}}\gamma_3'F_4^--\sqrt{\frac{3}{8}}C'k^+$ $+\frac{1}{\sqrt{8}}(\kappa''+1)H^-$	$\frac{1}{\sqrt{6}}Pk^-+\frac{1}{\sqrt{6}}GF_4^+$ $-\frac{1}{2}\sqrt{3}N_3H^+$	$-\frac{1}{2}\gamma_1k^2-\frac{1}{2}\gamma_2F_3^1$ $-\frac{1}{2}(\kappa+\frac{1}{4}q)H_z$		
$-N_2F_3^1+N_3H_z$	$-\frac{1}{2}\sqrt{3}Ck^+-\frac{3}{4}qH^-$	$-\frac{1}{2}\sqrt{3}\,\gamma_3F_4^+-\frac{1}{2}Ck^-$ $-\frac{1}{2}\sqrt{3}\,(\kappa+\frac{7}{4}q)H^+$	$-\sqrt{\frac{3}{8}}\,\gamma_3'F_4^+-\frac{1}{\sqrt{8}}C'k^-$ $-\sqrt{\frac{3}{8}}\,(\kappa''+1)H^+$	$-\frac{1}{\sqrt{2}}Pk^++\frac{1}{\sqrt{2}}GF_4^-$ $-\frac{1}{2}N_3H^-$	$\frac{1}{2}\gamma_2F_3^2+i\frac{1}{2}\sqrt{3}\,\gamma_3F_4^z$ $-Ck_z$	$-\frac{1}{2}\gamma_1k^2+\frac{1}{2}\gamma_2F_3^1$ $+\frac{3}{2}(\kappa+\frac{9}{4}q)H_z$	
$\frac{1}{\sqrt{3}}P'k_z+\frac{i}{\sqrt{3}}G'F_4^z$	$-\sqrt{\frac{3}{8}}\,\gamma_3'F_4^++\frac{1}{\sqrt{8}}C'k^-$ $+\sqrt{\frac{3}{8}}\,(\kappa''+1)H^+$	$\frac{3}{\sqrt{8}}\gamma_3'F_4^--\sqrt{\frac{3}{8}}C'k^+$ $-\frac{1}{\sqrt{8}}(\kappa''+1)H^-$	$-(\kappa'+\frac{1}{2})H^-$	$\frac{1}{\sqrt{3}}P'k^-+\frac{1}{\sqrt{3}}G'F_4^+$	$\frac{1}{\sqrt{2}}\gamma_2'F_3^1$ $-\frac{1}{\sqrt{2}}(\kappa''+1)H_z$	$\frac{1}{\sqrt{2}}\gamma_2'F_3^2$ $-i\frac{1}{2}\sqrt{6}\,\gamma_3'F_4^z$ $+\frac{1}{\sqrt{2}}C'k_z$	$-\Delta-\frac{1}{2}\gamma_1'k^2$ $-(\kappa'+\frac{1}{2})H_z$

will agree with the equations in the Appendix of Ref. 14, but the b-set matrix will have opposite signs in the off-diagonal elements of the last row and column. The states $|1\rangle - |8\rangle$ are identical with a set used by Groves, Pidgeon, Ewald, and Wagner,[21] except for a factor of (-1) in state $|6\rangle$. Thus the $J=\frac{3}{2}$ subset of Ref. 21 does *not* give the same matrices as those in Ref. 13.

Finally, the states $|1\rangle - |8\rangle$ differ from those of Pidgeon and Brown[12] and of Aggarwal.[16] Our results for the 8×8 $\vec{k}\cdot\vec{p}$ Hamiltonian will be related to those of Ref. 12 by a unitary transformation which is nearly the same as the one given by Aggarwal[16] from Reine's work.[22] The resulting 4×4 matrices for the a and b sets are real. Apart from overall factors, our states differ from those of Ref. 16 by a factor of (-1) for the states $|4\rangle$ and $|5\rangle$, which gives a factor of (-1) in the off-diagonal elements in the third row and third column of each 4×4 matrix.

As can be seen from the above discussion, our basis states are not identical to those of any of the important papers on InSb. However, it is also clear that this previous work involves several inconsistent basis sets. The considerations involved in choosing our set were: (i) to make the 4×4 matrices for the a and b sets real; (ii) to agree with the widely available KDWS tables[17]; and (iii) to agree with the most extensive previous work in the quasi-Ge model (a) Luttinger,[13] (b) Roth, Lax, and Zwerdling,[14] (c) Pidgeon and Brown,[12] and (d) Aggarwal.[16] Our set satisfies (i), (ii), and (iiia); it differs slightly from (iiib) to satisfy (ii), from (iiic) to satisfy (i), and from (iiid) to satisfy (iiia).

The character tables for the T_d group are given by Dresselhaus,[23] and by KDWS[17] on p. 88. It should be pointed out that the definition of Γ_4 and Γ_5 are reversed and that the column S_4 in Ref. 17 and $I\times C_4$ in Ref. 23 should have the same character, which means that the definitions of Γ_6 and Γ_7 are also reversed. The spin-$\frac{1}{2}$ basis set belongs to the KDWS Γ_7 or Dresselhaus Γ_6 representation. We will use the Dresselhaus notation. Using the KDWS tables of coupling coefficients for the T_d group, we find the matrices involving terms to second order in $\vec{k}$ among these basis functions. For example, two terms in $\vec{k}\times\vec{k}$ are $F_3^1 = 2k_z^2 - k_x^2 - k_y^2$ and $F_3^2 = \sqrt{3}\,(k_x^2 - k_y^2)$ which belongs to the two-fold Γ_3 representation. The matrix elements of these functions among the Γ_6, Γ_7, and Γ_8 states are proportional to the complex conjugates of the table entries on p. 91 of KDWS. The resulting matrices must be Hermitian and be invariant under time reversal. These conditions require certain parameters to be either zero or else purely real or imaginary.

All the real, independent parameters found in this manner are listed in Table I. We find matrices for all the previously defined parameters. The $\Gamma_8\times\Gamma_8$ parameters γ_1, γ_2, γ_3, κ, and q were defined by Luttinger.[13] γ_1, γ_2, γ_3, and κ were shown by Roth, Lax, and Zwerdling[14] also to involve the split-off band Γ_7 when one starts with single-group representations. In the full double-group picture the $\Gamma_7\times\Gamma_7$ and $\Gamma_7\times\Gamma_8$ parameters are independent of the $\Gamma_8\times\Gamma_8$ ones and are denoted by γ_1', γ_2', γ_3', κ', and κ''. The conduction-band (Γ_6) effective-mass parameter F, the "linear-k" parameter C for Γ_8 and the $\Gamma_6\times\Gamma_8$ parameters P and G were defined by Kane[18] and by Dresselhaus, Kip, and Kittel[20] in terms of single-group basis states; the $\Gamma_6\times\Gamma_7$ and $\Gamma_7\times\Gamma_8$ parameters are denoted by C', P', and G'. We also obtain three new parameters: N_1 contributes to the conduction-band g factor, similar to κ in the valence bands; N_2 and N_3 represent additional couplings between the Γ_6 conduction band and the Γ_8 valence bands. In the Appendix we show that these new parameters, like q, arise from the spin-orbit splitting of higher bands. The complete 8×8 matrix $\mathcal{H}$ for the parameters listed in Table I is given in Table II, which also includes the band-edge energies E_g and Δ relative to the Γ_8 valence band, and the parts of the free-electron terms not included in the definitions of γ_1 and κ.[14,16] Other terms used in Table II are

$$
\begin{aligned}
&k^2 \equiv k_x^2 + k_y^2 + k_z^2, \quad k^{\pm} \equiv k_x \pm i k_y, \\
&F_3^1 \equiv 2k_z^2 - k_x^2 - k_y^2, \quad F_3^2 \equiv \sqrt{3}\,(k_x^2 - k_y^2), \\
&F_4^{\pm} \equiv \{k_z, k^{\pm}\} \equiv (k_z k^{\pm} + k^{\pm} k_z), \quad F_4^{z} = \{k_x, k_y\}, \\
&H_z = i[k_x, k_y], \quad H^{\pm} = \pm[k^{\pm}, k_z].
\end{aligned}
\tag{2}
$$

For simplicity, Table II is given in atomic units $\hbar = m = 1$.

III. QUASI-GERMANIUM MODEL FOR $\vec{H}$ IN THE $(1\bar{1}0)$ PLANE

For a magnetic field $\vec{H}$ in the $(1\bar{1}0)$ plane at an angle θ from the z axis, we perform the coordinate transformation given by Luttinger[13]

$$
\begin{aligned}
k_x &= 1/\sqrt{2}\,(ck_1 - k_2 + sk_3), \\
k_y &= 1/\sqrt{2}\,(ck_1 + k_2 + sk_3), \\
k_z &= -sk_1 + ck_3,
\end{aligned}
$$

where $s \equiv \sin\theta$, $c \equiv \cos\theta$. The coordinate axes are labeled 1, 2, and 3, where $\vec{H}$ is along the three axis, and the two axis is the $[1\bar{1}0]$ crystal axis. The corresponding rotation of the basis states results in a transformation of the $\vec{k}\cdot\vec{p}$ Hamiltonian according to $\mathcal{H}(\theta) = U_\theta^{\dagger}\mathcal{H}U_\theta$.[9] We then set

$$k_1=\frac{1}{\lambda\sqrt{2}}(a+a^+),\quad k_2=\frac{i}{\lambda\sqrt{2}}(a-a^+),\quad k_3\equiv k_H,\qquad (4)$$

where $\lambda\equiv(\hbar c_0/eH)^{1/2}$ is the Landau radius, c_0 is the velocity of light, $\hbar k_H$ is the component of the momentum along the direction of the applied magnetic field, and a^+, a are raising and lowering operators for harmonic-oscillator functions ϕ_n

$$a^{\pm}\phi_n=(n+1)^{1/2}\phi_{n+1},\quad a\phi_n=\sqrt{n}\,\phi_{n-1},$$
$$N\phi_n\equiv a^+a\phi_n=n\phi_n,\qquad (5)$$

and

$$[a,a^+]\equiv aa^+-a^+a=1.\qquad (6)$$

The resulting $\mathcal{H}(\theta)$ separates into two 4×4 matrices for the a and b sets

$$\mathcal{H}(\theta)\approx\begin{pmatrix}\mathcal{H}_a & 0\\ 0 & \mathcal{H}_b\end{pmatrix}\qquad (7)$$

if one neglects terms proportional to k_H, q, C, G, N_2, and N_3 and most terms proportional to the warping parameter $\mu\equiv\frac{1}{2}(\gamma_3-\gamma_2)$. One can include some warping by way of two valence-band effective mass parameters[13]

$$\gamma'\equiv\gamma_3+(\gamma_2-\gamma_3)\left(\frac{3c^2-1}{2}\right)^2,$$
$$\gamma''\equiv\tfrac{1}{3}\gamma_2+\tfrac{2}{3}\gamma_3+\tfrac{1}{6}(\gamma_2-\gamma_3)\left(\frac{3c^2-1}{2}\right)^2,\qquad (8)$$

where, again $c\equiv\cos\theta$. The resulting 4×4 matrices $\mathcal{H}_a$ and $\mathcal{H}_b$ are displayed in Table III, where the terms involving γ_1, γ', and γ'' in the fourth rows and columns are included in the single-group approximation $P'\simeq P$, $\gamma_1'\simeq\gamma_1$, etc. Also in Table III, P is included using the interband energy $E_p\equiv2mP^2/\hbar^2$, and $\mu_B\equiv e\hbar/2mc_0$ is the Bohr magneton. Table III is now in ordinary energy units since E_g, Δ, E_p, and μ_BH have the dimensions of energy and F, K, N_1, and the γ's are dimensionless.

The Hamiltonians of Table III are equivalent[24] to those of Pidgeon and Brown[12] [their Eqs. (10) and (11)] when account is taken of the different basis sets. Table III is also equivalent to Eqs. (B9) and (B10) of Roth, Lax, and Zwerdling[14] for the Γ_8 and Γ_7 band energies except, as indicated above, for a sign change in the matrix elements involving the Γ_7, b-set state.

The solutions to the Schrödinger equations $\mathcal{H}_a|a\rangle=E_a|a\rangle$ and $\mathcal{H}_b|b\rangle=E_b|b\rangle$ are of the form

$$|a(n)\rangle=\begin{bmatrix}a_1^n\phi_n\\ a_3^n\phi_{n-1}\\ a_5^n\phi_{n+1}\\ a_7^n\phi_{n+1}\end{bmatrix},\quad |b(n)\rangle=\begin{bmatrix}b_2^n\phi_n\\ b_6^n\phi_{n-1}\\ b_4^n\phi_{n+1}\\ b_8^n\phi_{n-1}\end{bmatrix}\qquad (9)$$

with $n\geq-1$ and with $a_1^{-1}=b_2^{-1}=a_3^{-1}=a_3^0=b_6^{-1}=b_6^0=b_8^{-1}=b_8^0\equiv0$. For $n\geq1$, there are eight independent solutions $|a(n)\rangle$, $|b(n)\rangle$ for each n, which are denoted, in order of decreasing energy, conduction band $[|a^c(n)\rangle, |b^c(n)\rangle]$, heavy hole $[|a^-(n)\rangle, |b^-(n)\rangle]$, light hole $[|a^+(n)\rangle, |b^+(n)\rangle]$, and split-off band $[|a^s(n)\rangle, |b^s(n)\rangle]$. Pidgeon and Brown[12] renumbered all valence-band states $n\to n+1$; since we are concerned with conduction-band states only, such renumbering is unnecessary. Although a number of authors[13,14,25] have given approximate analytical solutions for the states $|a(n)\rangle$, $|b(n)\rangle$ and the corresponding energies $E_a(n), E_b(n)$, the numerical solutions obtained by Pidgeon and Brown[12] were necessary to give an accurate fit to their interband magneto-optical experiments in InSb.

The strongest allowed optical transitions among the states of Eqs. (9) are those proportional to the interband matrix element P; that is, we find the optical perturbation $\mathcal{H}_\omega'$ by replacing $\vec{k}$ by $(\vec{k}+e\vec{A}/\hbar c)$ in the matrix for P, where $\vec{A}$ is the light-vector potential in the radiation gauge. The resulting transition-matrix elements are

$$\langle a(n')|\mathcal{H}_\omega'(P)|a(n)\rangle=\frac{eE}{2\omega}\left(\frac{E_p}{6m}\right)^{1/2}\{[\sqrt{3}\,a_3^{n'}a_1^n-a_1^{n'}(a_5^n-\sqrt{2}\,a_7^n)]\hat{\epsilon}_-\delta_{n',n+1}+(n\to n')\hat{\epsilon}_+\delta_{n',n-1}\}$$
$$\langle b(n')|\mathcal{H}_\omega'(P)|b(n)\rangle=\frac{eE}{2\omega}\left(\frac{E_p}{6m}\right)^{1/2}\{[(b_6^{n'}+\sqrt{2}\,b_8^{n'})b_2^n-\sqrt{3}\,b_2^{n'}b_4^n]\hat{\epsilon}_-\delta_{n',n+1}+(n\to n')\hat{\epsilon}_+\delta_{n',n-1}\},\qquad (10)$$
$$\langle b(n')|\mathcal{H}_\omega'(P)|a(n)\rangle=-\frac{eE}{\omega}\left(\frac{E_p}{6m}\right)^{1/2}[b_2^{n'}(\sqrt{2}\,a_5^n+a_7^n)+(\sqrt{2}\,b_6^{n'}-b_8^na_1^n)]\hat{\epsilon}_3\delta_{n',n+1},$$

where E is the optical electric field. $\hat{\epsilon}_+$ and $\hat{\epsilon}_-$ are the unit polarization vectors for, respectively, right and left circular polarization σ_R, σ_L transverse to the magnetic field $\vec{H}$, and $\hat{\epsilon}_3$ is a unit polarization vector parallel to $\vec{H}$ usually referred to as the π or $\vec{E}\parallel\vec{H}$ polarization. Thus the selection rules for both inter- and intraband transitions (before renumbering of the valence bands) are

TABLE III. Quasi-Ge model for InSb: separate Hamiltonians for the a and b sets of Landau levels, for a magnetic field in the $(1\bar{1}0)$ plane.

$\mathcal{H}_a =$

$\lvert 1\rangle$	$\lvert 3\rangle$	$\lvert 5\rangle$	$\lvert 7\rangle$
$E_g + 2[F(2N+1) + N_1 + N + 1]\mu_B H$	$(\mu_B H E_p)^{1/2} a^+$	$-\left(\frac{\mu_B H E_p}{3}\right)^{1/2} a$	$\left(\frac{2\mu_B H E_p}{3}\right)^{1/2} a$
$(\mu_B H E_p)^{1/2} a$	$-[(\gamma_1+\gamma')(2N+1)+3\kappa]\mu_B H$	$2\sqrt{3}\,\mu_B H\gamma'' a^2$	$-2\sqrt{6}\,\mu_B H\gamma'' a^2$
$-\left(\frac{\mu_B H E_p}{3}\right)^{1/2} a^+$	$2\sqrt{3}\,\mu_B H\gamma'' a^{+2}$	$-[(\gamma_1-\gamma')(2N+1)-\kappa]\mu_B H$	$\sqrt{2}\,[\gamma'(2N+1)-\kappa-1]\mu_B H$
$\left(\frac{2\mu_B H E_p}{3}\right)^{1/2} a^+$	$-2\sqrt{6}\,\mu_B H\gamma'' a^{+2}$	$\sqrt{2}\,[\gamma'(2N+1)-\kappa-1]\mu_B H$	$-\Delta-[\gamma_1(2N+1)-2\kappa-1]\mu_B H$

$\mathcal{H}_b =$

$\lvert 2\rangle$	$\lvert 6\rangle$	$\lvert 4\rangle$	$\lvert 8\rangle$
$E_g + 2[F(2N+1) - N_1 + N]\mu_B H$	$\left(\frac{\mu_B H E_p}{3}\right)^{1/2} a$	$-(\mu_B H E_p)^{1/2} a$	$\left(\frac{2\mu_B H E_p}{3}\right)^{1/2} a^+$
$\left(\frac{\mu_B H E_p}{3}\right)^{1/2} a$	$-[(\gamma_1-\gamma')(2N+1)+\kappa]\mu_B H$	$2\sqrt{3}\,\mu_B H\gamma'' a^2$	$-\sqrt{2}\,[\gamma'(2N+1)+\kappa+1]\mu_B H$
$-(\mu_B H E_p)^{1/2} a^+$	$2\sqrt{3}\,\mu_B H\gamma'' a^{+2}$	$-[(\gamma_1+\gamma')(2N+1)-3\kappa]\mu_B H$	$2\sqrt{6}\,\mu_B H\gamma'' a^{+2}$
$\left(\frac{2\mu_B H E_p}{3}\right)^{1/2} a$	$-\sqrt{2}\,[\gamma'(2N+1)+\kappa+1]\mu_B H$	$2\sqrt{6}\,\mu_B H\gamma'' a^2$	$-\Delta-[\gamma_1(2N+1)+2\kappa+1]\mu_B H$

$$\begin{aligned}
&\sigma_L: a_n \to a_{n+1}, \quad b_n \to b_{n+1}, \\
&\sigma_R: a_n \to a_{n-1}, \quad b_n \to b_{n-1}, \\
&\pi: \ a_n \to b_{n+1}, \quad b_n \to a_{n-1}.
\end{aligned} \tag{11}$$

For intraband transitions, the σ_L transition occurs at the cyclotron frequency $\omega = \omega_c$, and the π transition at the "combined resonance" frequency $\omega = \omega_c + \omega_s$, where ω_s is the spin-flip frequency.

IV. WARPING AND INVERSION ASYMMETRY PERTURBATIONS

The terms not included in the quasi-Ge Hamiltonian of Table III divide into three categories: (i) terms proportional to k_H and k_H^2; (ii) the so-called warping terms proportional to $\mu = \frac{1}{2}(\gamma_3 - \gamma_2)$ and q, both considered by Luttinger[13]; and (iii) the inversion-asymmetry terms proportional to C, G, and the new parameters N_2 and N_3. All of these extra terms are given in Table IV. The terms involving k_H are proportional to the effective mass parameters F, γ_1, and γ', and to

$$\gamma''' \equiv \tfrac{2}{3}\gamma_2 + \tfrac{1}{3}\gamma_3 - \tfrac{2}{3}(\gamma_2 - \gamma_3)\left(\frac{3c^2-1}{2}\right)^2 . \tag{12}$$

The warping terms are proportional to

$$\begin{aligned}
\mu_1 &\equiv -\tfrac{3}{2}\mu\mu_B H(3c^2-1)[s^2(a^2 + a^{+2}) - 2\sqrt{2}\,sc\lambda k_H(a + a^+)] \\
\mu_2 &\equiv \tfrac{1}{2}\sqrt{3}\,\mu\mu_B H\{s^2(3c^2-1)(2N+1-2\lambda^2 k_H^2) - (c^2-3)(3c^2-1)a^2 + 2\sqrt{2}\,sc\lambda k_H[(5-3c^2)a - (3c^2-1)a^+]\}, \\
\mu_3 &\equiv -\sqrt{3}\,\mu\mu_B H\{sc[(3c^2-1)(2N+1-2\lambda^2 k_H^2) - (5-3c^2)a^2 + (3c^2-1)a^{+2}] + 2\sqrt{2}\,s^2(3c^2-1)\lambda k_H a\},
\end{aligned} \tag{13}$$

and to

$$\begin{aligned}
q_1 &\equiv -\tfrac{3}{4} q\mu_B H(3c^4 - 2c^2 + 8), \\
q_2 &\equiv -\tfrac{3}{4}\sqrt{3}\, q\mu_B H s^2(3c^2-1), \\
q_3 &\equiv \tfrac{3}{4}\sqrt{3}\, q\mu_B H sc(3c^2-1), \\
q_4 &\equiv -\tfrac{3}{4} q\mu_B H sc(3c^2-5), \\
q_5 &\equiv -\tfrac{1}{4} q\mu_B H(27c^4 - 18c^2 - 10), \\
q_6 &\equiv -\tfrac{9}{8}\, q\mu_B H sc(3c^2-1).
\end{aligned} \tag{14}$$

The terms from Eqs. (13) and (14) in the $\Gamma_8 \times \Gamma_8$ portions of Table IV (involving states $|3\rangle - |6\rangle$) are identical to those given by Luttinger,[13] but with the opposite signs throughout, since Luttinger's equations involved hole energies. Table IV includes additional couplings proportional to μ between the Γ_8 and Γ_7 bands.

The inversion-asymmetry terms are proportional to

$$\begin{aligned}
c_1 &\equiv \tfrac{1}{8}\sqrt{6}\,\frac{C}{\lambda}\, s(3c^2-1)(a - a^+), \\
c_2 &\equiv \tfrac{1}{8}\sqrt{2}\,\frac{C}{\lambda}\,[5s(3c^2-1)a^+ - 3s(1+c^2)a \\
&\qquad - 2\sqrt{2}\, c(3c^2-1)\lambda k_H], \\
c_3 &\equiv \tfrac{1}{8}\sqrt{2}\,\frac{C}{\lambda}\,[12s^2 c a^+ + 2c(3c^2-1)a \\
&\qquad - \sqrt{2}\, s(3c^2-1)\lambda k_H], \\
c_4 &\equiv \tfrac{1}{8}\sqrt{6}\,\frac{C}{\lambda}\,[2c(3c^2-1)a^+ + 3\sqrt{2}\, s(1+c^2)\lambda k_H], \\
c_5 &\equiv \tfrac{1}{4}\,\frac{C}{\lambda}\,[s(3c^2-1)a^+ + 3s(1+c^2)a \\
&\qquad - \sqrt{2}\, c(3c^2-1)\lambda k_H], \\
c_6 &\equiv -\tfrac{1}{4}\sqrt{3}\,\frac{C}{\lambda}\,[s(3c^2-1)(a + a^+) + 3\sqrt{2}\, s^2 c\lambda k_H], \\
c_7 &\equiv \tfrac{1}{4}\,\frac{C}{\lambda}\,[3s^2 c a^+ - c(3c^2-1)a \\
&\qquad - \sqrt{2}\, s(3c^2-1)\lambda k_H],
\end{aligned} \tag{15}$$

and to

TABLE IV. Terms in 8×8 Hamiltonian $\mathcal{H}'$ neglected in Table III. See Eqs. (12) through (18) for definitions of terms. The upper triangle is the Hermitian conjugate of the lower one.

$\|1\rangle$	$\|3\rangle$	$\|5\rangle$	$\|7\rangle$	$\|2\rangle$	$\|6\rangle$	$\|4\rangle$	$\|8\rangle$
$(F+\frac{1}{2})\frac{\hbar^2}{m}k_H^2$							
$i(g_1+e_1+f_1)$	$-(\gamma_1-2\gamma')\frac{\hbar^2}{2m}k_H^2$						
	$+\mu_1+q_1+ic_1$						
$i\sqrt{3}\,(-\frac{1}{3}g_1^\dagger-e_1^\dagger-f_1)$	$\mu_2+q_2+ic_2$	$-(\gamma_1+2\gamma')\frac{\hbar^2}{2m}k_H^2$					
		$-\mu_1+q_5+3ic_1$					
$i\sqrt{\frac{2}{3}}\,g_1^\dagger$	$-\sqrt{2}\,\mu_2+ic_5$	$-\sqrt{2}\,\gamma'\frac{\hbar^2}{m}k_H^2$	$-\gamma_1\frac{\hbar^2}{2m}k_H^2$				
		$-\sqrt{2}\,\mu_1+ic_6$					
0	$-i(e_3-f_3)$	$-\left(\frac{2\mu_B HE_p}{3}\right)^{1/2}\lambda k_H$	$-\left(\frac{\mu_B HE_p}{3}\right)^{1/2}\lambda k_H-\frac{i}{\sqrt{2}}g_2$	$(F+\frac{1}{2})\frac{\hbar^2}{m}k_H^2$			
		$-i(g_2+e_2-f_2)$					
$-\left(\frac{2\mu_B HE_p}{3}\right)^{1/2}\lambda k_H$	$2\sqrt{6}\,\gamma'''\mu_B H\lambda k_H a^+$	$q_6+i\sqrt{3}\,c_3^\dagger$	$6\gamma'''\mu_B H\lambda k_H a$	$i\sqrt{3}\,(\frac{1}{3}g_1-e_1-f_1)$	$-(\gamma_1+2\gamma')\frac{\hbar^2}{2m}k_H^2$		
$+i(g_2+e_2+f_2)$	$+\mu_3+q_3+ic_3$		$+\sqrt{\frac{3}{2}}\,\mu_3^\dagger+i\sqrt{3}\,c_7^\dagger$		$-\mu_1-q_5-3ic_1$		
$i(e_3+f_3)$	q_4+ic_4	$-2\sqrt{6}\,\gamma'''\mu_B H\lambda k_H a^+$	$-2\sqrt{3}\,\gamma'''\mu_B H\lambda k_H a^+$	$-i(g_1^\dagger+e_1^\dagger-f_1)$	$\mu_2-q_2-ic_2$	$-(\gamma_1-2\gamma')\frac{\hbar^2}{2m}k_H^2$	
		$-\mu_3+q_3+ic_3$	$-\frac{1}{\sqrt{2}}\,\mu_3-ic_7$			$+\mu_1-q_1-ic_1$	
$\left(\frac{\mu_B HE_p}{3}\right)^{1/2}\lambda k_H-\frac{i}{\sqrt{2}}g_2$	$-2\sqrt{3}\,\gamma'''\mu_B H\lambda k_H a^+$	$6\gamma'''\mu_B H\lambda k_H a$	0	$i\sqrt{\frac{2}{3}}\,g_1$	$\sqrt{2}\,\gamma'\frac{\hbar^2}{m}k_H^2$	$\sqrt{2}\,\mu_2^\dagger-ic_5^\dagger$	$-\gamma_1\frac{\hbar^2}{2m}k_H^2$
	$-\frac{1}{\sqrt{2}}\mu_3+ic_7$	$+\sqrt{\frac{3}{2}}\,\mu_3^\dagger-i\sqrt{3}\,c_7^\dagger$			$+\sqrt{2}\,\mu_1-ic_6$		

$$g_1 \equiv \frac{G\mu_B H}{\sqrt{2}}\left[-s(3c^2-1)(2N+1-2\lambda^2k_H^2+a^2)\right.$$
$$-3s(1+c^2)a^{+2}-6\sqrt{2}\,s^2c\lambda k_H a$$
$$\left.+2\sqrt{2}\,c(3c^2-1)\lambda k_H a^+\right],$$
$$g_2 \equiv \frac{2G\mu_B H}{\sqrt{6}}\left[3s^2c(2N+1-2\lambda^2k_H^2)\right. \tag{16}$$
$$-c(3c^2-1)(a^2+a^{+2})$$
$$\left.-2\sqrt{2}\,s(3c^2-1)\lambda k_H(a+a^+)\right];$$

$$e_1 \equiv \tfrac{1}{2}N_2\mu_B H\left[-s(3c^2-1)(2N+1-2\lambda^2k_H^2+3a^2)\right.$$
$$\left.+3s(1+c^2)a^{+2}-12\sqrt{2}\,s^2c\lambda k_H a\right],$$

$$e_2 \equiv -\sqrt{3}\,N_2\mu_B H\left[c(3c^2-1)(a^2-a^{+2})\right. \tag{17}$$
$$\left.+\sqrt{2}\,s(3c^2-1)\lambda k_H(a-a^+)\right],$$

$$e_3 \equiv -N_2\mu_B H\left[c(3c^2-1)(2N+1-2\lambda^2k_H^2)-6s^2ca^{+2}\right.$$
$$\left.+3\sqrt{2}\,s(1+c^2)\lambda k_H a+3\sqrt{2}\,s(3c^2-1)\lambda k_H a^+\right];$$

$$f_1 \equiv N_3\mu_B Hs(3c^2-1),\quad f_2 \equiv -3\sqrt{3}\,N_3\mu_B Hs^2c, \tag{18}$$
$$f_3 \equiv -N_3\mu_B Hc(3c^2-1).$$

This rotation in the $(1\bar{1}0)$ plane includes the three important directions $\vec{H}\|[001]$, $[110]$, and $[111]$. The portions of the matrix in Table IV for couplings within the Γ_8 band proportional to C [Eqs. (15)] for these three orientations, and for $k_H=0$, are the same as those given by Pidgeon and Groves[11] with an overall sign change since they, like Luttinger,[13] consider hole energies. Similarly, their result for couplings proportional to q for $\vec{H}\|[111]$ is identical to ours [Eqs. (14)] with the sign reversed. However, our result for μ [Eqs. (13)] for $\vec{H}\|[111]$ is identical to that of Pidgeon and Groves with no sign change, so that their results for the μ matrix differ in sign from that of Luttinger. Our results, as indicated above, agree with that of Luttinger with an overall sign change.

V. SELECTION RULES FOR CYCLOTRON-HARMONIC TRANSITIONS

Bell and Rogers[8] calculated transition strengths for intraband optical transitions, for $\vec{H}\|[001]$ only, by diagonalizing the Hamiltonian of Table III in the single-group basis set, without the parameter q and the new parameters N_1, N_2, and N_3. Because this Hamiltonian couples an infinitely large number of oscillator functions φ_n, they obtained numerical solutions by diagonalizing two 120×120 truncated matrices. In addition to the fundamental cyclotron resonance ω_c for the σ_L polarization and the combined resonance $\omega_c+\omega_s$ for the π polarization, they found that the following intraconduction-band optical transitions were weakly allowed

$$\begin{aligned}
&\sigma_L\colon\ a_n \to b_n\ (\omega_s)\\
&\qquad b_n \to a_{n+2}\ (2\omega_c-\omega_s),\\
&\sigma_R\colon\ a_n \to b_{n+2}\ (2\omega_c+\omega_s)\\
&\qquad a_n \to a_{n+3}\ (3\omega_c),\\
&\pi\colon\ a_n \to a_{n+2}\ (2\omega_c)\\
&\qquad b_n \to a_{n+3}\ (3\omega_c-\omega_s).
\end{aligned} \tag{19}$$

TABLE V. Couplings among the quasi-Ge states of Eq. (9), proportional to the warping parameters μ and q and the inversion-asymmetry parameters C, G, N_2, and N_3 for $k_H=0$ and extra couplings for $k_H\neq0$.

		$k_H=0$	$k_H\neq0$
$\vec{H}\|[001]$	μ	$a_n\cdots a_{n\pm4}$ $b_n\cdots b_{n\pm4}$	
	q		
	C	$a_n\cdots b_{n-1}, b_{n+3}$	$a_n\cdots a_{n\pm2}$ $b_n\cdots b_{n\pm2}$
	G	$a_n\cdots b_{n-1}, b_{n+3}$	$a_n\cdots a_{n\pm2}$ $b_n\cdots b_{n\pm2}$
	N_2	$a_n\cdots b_{n-1}, b_{n+3}$	
	N_3	$a_n\cdots b_{n-1}$	
$\vec{H}\|[110]$	μ	$a_n\cdots a_{n\pm2}, a_{n\pm4}$ $b_n\cdots b_{n\pm2}, b_{n\pm4}$	$a_n\cdots b_{n-1}, b_{n+3}$
	q	$a_n\cdots a_{n\pm2}$ $b_n\cdots b_{n\pm2}$	
	C	$a_n\cdots a_{n\pm1}, a_{n\pm3}$ $b_n\cdots b_{n\pm1}, b_{n\pm3}$	$a_n\cdots b_{n-2}, b_n, b_{n+2}$
	G	$a_n\cdots a_{n\pm1}, a_{n\pm3}$ $b_n\cdots b_{n\pm1}, b_{n\pm3}$	$a_n\cdots b_n, b_{n+2}$
	N_2	$a_n\cdots a_{n\pm1}, a_{n\pm3}$ $b_n\cdots b_{n\pm1}, b_{n\pm3}$	$a_n\cdots b_{n-2}, b_n, b_{n+2}$
	N_3	$a_n\cdots a_{n\pm1}$ $b_n\cdots b_{n\pm1}$	
$\vec{H}\|[111]$	μ	$a_n\cdots b_{n-2}, b_{n+1}$	$a_n\cdots a_{n\pm3}$ $b_n\cdots b_{n\pm3}$
	q	$a_n\cdots b_{n-2}$	
	C	$a_n\cdots a_{n\pm3}$ $a_n\cdots b_{n+1}$ $b_n\cdots b_{n\pm3}$	$a_n\cdots b_{n-2}$
	G	$a_n\cdots a_{n\pm3}$ $a_n\cdots b_{n+1}$ $b_n\cdots b_{n\pm3}$	
	N_2	$a_n\cdots a_{n\pm3}$ $a_n\cdots b_{n+1}$ $b_n\cdots b_{n\pm3}$	$a_n\cdots b_{n-2}$
	N_3	$a_n\cdots b_{n+1}$	

They showed that these were the result of warping- and inversion-asymmetry effects. We use a perturbation treatment to find the intraband selection rules for $\vec{H}\|[110]$, and [111] as well as [001], as outlined below.

Using the Hamiltonian $\mathcal{H}'$ in Table IV as a perturbation in the basis states of Eq. (9), we find new states

$$|a'(n)\rangle = |a(n)\rangle + \sum_{n'} \sum_{j=a,b} \frac{\langle j(n')|\mathcal{H}'|a(n)\rangle}{E(j(n)') - E(a(n))} |j(n')\rangle \ . \tag{20}$$

And similarly for $|b'(n)\rangle$, where we consider only conduction-band states $a=a^c$ and $b=b^c$, and coupled state $j=a^c$, b^c. Since the couplings of Eq. (20) are all very small compared to the energy differences, it was not necessary to include the energy corrections. The actual expressions for these couplings are very lengthy. All such couplings, proportional to the warping- and inversion-asymmetry parameter, are summarized in Table V.

Using these coupled states, the allowed optical transitions originating in the state $a(n)$ are proportional to the square of the matrix element $\langle f'(n')|\mathcal{H}'_\omega|a'(n)\rangle$ which becomes

$$\langle f'(n')|\mathcal{H}'_\omega|a'(n)\rangle = \langle f(n')|\mathcal{H}'_\omega|a(n)\rangle + \sum_{n''} \sum_{j=a,b} \left(\frac{\langle f(n')|\mathcal{H}'_\omega|j(n'')\rangle\langle j(n'')|\mathcal{H}'|a(n)\rangle}{E(j(n'')) - E(a(n))} + \frac{\langle f(n')|\mathcal{H}'|j(n'')\rangle\langle j(n'')|\mathcal{H}'_\omega|a(n)\rangle}{E(f(n')) - E(j(n''))} \right), \tag{21}$$

with a similar expression for transitions originating in the state $b(n)$. The summation runs over all intermediate states in the conduction band. The first term in Eq. (21) represents an "allowed" transition. The matrix elements of $\mathcal{H}'_\omega$ proportional to P are given in Eqs. (10). These and all other matrix elements are calculated using the approximate numerical solutions [Eqs. (9)] to the quasi-Ge Hamiltonians in Table III.

The intraconduction-band transitions allowed in Eq. (21) by the couplings in Table V are listed in Table VI. We use the notation of Eq. (19): a transition from a_n to a_{n+m} is denoted by $m\omega_c$; from a_n to b_{n+m} by $m\omega_c+\omega_s$, and from b_n to a_{n+m} by $m\omega_c-\omega_s$. We would like to point out again that, in fact, the conduction-band Landau levels

TABLE VI. Intraconduction-band transitions in InSb for a magnetic field $\vec{H}\|[001]$, [110], and [111] crystal axes, for $k_H=0$ and extra transitions for $k_H\neq 0$, for optical polarizations σ_L, σ_R, and π, both allowed (A) and induced by warping (W) and inversion asymmetry (I).

		$k_H=0$			$k_H\neq 0$		
		σ_L	σ_R	π	σ_L	σ_R	π
All orientations	A	ω_c	...	$\omega_c+\omega_s$	$2\omega_c+\omega_s$	ω_s	...
$\vec{H}\|[001]$	W	$5\omega_c$	$3\omega_c$	$3\omega_c-\omega_s$, $5\omega_c+\omega_s$	...	...	...
	I	ω_s, $2\omega_c-\omega_s$, $4\omega_c+\omega_s$	$2\omega_c+\omega_s$	$2\omega_c$	$3\omega_c$	ω_c	$\omega_c-\omega_s$, $3\omega_c+\omega_s$
$\vec{H}\|[110]$	W	$3\omega_c$, $5\omega_c$	ω_c, $3\omega_c$	$\omega_c-\omega_s$, $3\omega_c\pm\omega_s$, $5\omega_c+\omega_s$	ω_s, $2\omega_c-\omega_s$, $4\omega_c+\omega_s$	$2\omega_c+\omega_s$	$2\omega_c$
	I	$2\omega_c$, $4\omega_c$	$2\omega_c$	ω_s, $2\omega_c\pm\omega_s$, $4\omega_c+\omega_s$	$\omega_c\pm\omega_s$, $3\omega_c\pm\omega_s$	$\omega_c\pm\omega_s$	ω_c, $3\omega_c$
$\vec{H}\|[111]$	W	$3\omega_c-\omega_s$, $5\omega_c+\omega_s$	$\omega_c-\omega_s$, $3\omega_c+\omega_s$	$3\omega_c$	$4\omega_c$	$2\omega_c$	$2\omega_c-\omega_s$, $4\omega_c+\omega_s$
	I	$2\omega_c+\omega_s$, $4\omega_c$	ω_s, $2\omega_c$	$2\omega_c-\omega_s$, $4\omega_c+\omega_s$	$3\omega_c-\omega_s$	$\omega_c-\omega_s$	$3\omega_c$

are not equally spaced, so that the transitions are not precisely harmonic transitions; we use the $m\omega_c$ notation for convenience. In Table VI we have grouped together the transitions induced by warping (μ and q) and by inversion asymmetry (C, G, N_2, N_3) and have included the allowed transitions as well. For $\vec{H} \| [001]$ and $k_H = 0$ our results are consistent with those of Bell and Rogers,[8] summarized in Eq. (19).

A calculation of selection rules for the cyclotron-harmonic transitions has recently been made for the $\vec{H} \| [001]$ orientation by Zawadzki and Wlasak.[10] Their analysis includes transitions proportional to the parameters μ, C, and G, but not q, N_2, or N_3. Their perturbation treatment is similar to ours, but includes some weak transitions allowed to second order in the warping, inversion-asymmetry, and $k_H \neq 0$ effects. Zawadzki and Wlasak obtain for $\vec{H} \| [001]$ the transitions we list in Table VI, and, in addition, other transitions: $6\omega_c(\pi)$, $4\omega_c \pm \omega_s$, and $8\omega_c \pm \omega_s$ (σ_L and σ_R) allowed by a combination of μ and C effects, and also $4\omega_c(\pi)$, $2\omega_c \pm \omega_s$, and $6\omega_c \pm \omega_s$ (σ_L and σ_R) allowed by μ and $k_H \neq 0$. We expect these transitions, which arise only in a third-order perturbation treatment, to be considerably weaker than those in Table VI.

Our quantum-mechanical calculation confirms the results of Zeiger, Lax, and Dexter,[19] who obtained the intensities of the harmonics of heavy-hole cyclotron resonance in Ge and Si from a semiclassical Boltzman treatment. They found that the third-harmonic intensity should be zero for $\vec{E} \perp \vec{H} \| [111]$ and for $\vec{E} \| \vec{H} \| [001]$ and $[110]$, and the second-harmonic intensity, allowed for $k_H \neq 0$, should be zero for $\vec{E} \perp \vec{H} \| [001]$ and $[110]$ and for $\vec{E} \| \vec{H} \| [001]$ and $[111]$; these selection rules are consistent with Table VI, where $\vec{E} \perp \vec{H}$ induces both σ_L and σ_R transitions.

VI. COMPARISON WITH EXPERIMENTS

Experimentally, only the lowest-energy harmonic transitions $2\omega_c$, $2\omega_c + \omega_s$, and $3\omega_c$, from the ground state $a^c(0)$, have been identified.[1-5] The experimental results of Favrot *et al.*[5] are compared in Table VII with the results in Table VI for $k_H = 0$. As can be seen, the predicted selection rules for these transitions are confirmed experimentally, with one important exception. Favrot *et al.* observed a strong transition at $2\omega_c$ for $\vec{E} \perp \vec{H} \| [001]$ which is not explained by our calculations, even for $k_H \neq 0$. They also found very weak absorptions in the $\vec{E} \| \vec{H}$ polarization, for example, $3\omega_c$ for $\vec{H} \| [110]$, and somewhat stronger absorptions at $2\omega_c + \omega_s$ for $\vec{H} \| [001]$ and $[111]$ axes, which are not yet understood. It is evident from the spectra of Ref. 5 that population effects ($k_H \neq 0$) are not important, since the strongest $k_H \neq 0$ line predicted in Table VI, $2\omega_c + \omega_s$ for $\vec{E} \perp \vec{H}$ in all orientations, is not observed for $\vec{E} \perp \vec{H} \| [110]$. The results of Favrot *et al.*[5] were recently confirmed over the wavelength region ~7.5 to 18 μm by K. Lee,[26] for $\vec{H} \| [110]$ and $[111]$ axes, except that Lee did not observe the weak $2\omega_c + \omega_s$ line for $\vec{E} \| \vec{H} \| [111]$.

A calculation by Miyake[27] of impurity cyclotron-resonance harmonics suggests a possible explanation for the $2\omega_c$, $\vec{E} \perp \vec{H} \| [001]$ transition observed by Favrot *et al.*[5] If the ground-state electron occupies an impurity state associated with the $a^c(0)$ Landau level, the impurity potential acts as a perturbation which allows the electron to make transitions to all $a^c(n)$ levels, $n \geq 1$. Miyake's calculations indicate that the strongest harmonic is the second ($n = 2$ or $2\omega_c$), about 10 times stronger than the third harmonic. Thus the impurity potential could have a strong effect on the $2\omega_c$ absorption but have only a small effect on the $3\omega_c$ absorption. However, the impurity-induced coupling $a^c(n) \cdots a^c(n')$ and $b^c(n) \cdots b^c(n')$ cannot induce the $2\omega_c + \omega_s$, $\vec{E} \perp \vec{H}$ transitions or the $2\omega_c$ and $3\omega_c$ $\vec{E} \| \vec{H}$ transitions listed in Table VII.

McCombe *et al.*[28] observed cyclotron resonance absorption at ω_c as well as the harmonics $2\omega_c$ and $3\omega_c$ in n-type InSb for the "inactive" sense of circular polarization σ_R. They interpreted these results, particularly the position shift of the harmonics with carrier density, in terms of electron-plasmon interaction. This interpretation was disputed by Blinowski and Mycielski[29] and defended by Quinn *et al.*[30] These may also have a contribution from inversion-asymmetry effects. McCombe, *et al.*[28] do not specify the sample orientation; if they had $\vec{H} \| [110]$ one would predict from the couplings in Table V for $k_H = 0$, weak transitions for σ_L at $2\omega_c$, $3\omega_c$, $4\omega_c$, and $5\omega_c$, and for σ_R at ω_c, $2\omega_c$, and $3\omega_c$. The σ_L transitions were evidently obscured by the overabsorbed cyclotron-resonance transition, but the σ_R transitions follow these selection rules.

TABLE VII. Comparison of the theoretical selection rules for $k_H = 0$ for the lowest-energy harmonic transitions $2\omega_c$, $2\omega_c + \omega_s$, and $3\omega_c$, with the experimental results of Favrot, Aggarwal, and Lax.[5]

		$\vec{E} \perp \vec{H}$	$\vec{E} \| \vec{H}$
$\vec{H} \| [001]$	Theory	$2\omega_c + \omega_s, 3\omega_c$	$2\omega_c$
	Exp.	$2\omega_c, 2\omega_c + \omega_s, 3\omega_c$	$2\omega_c$
$\vec{H} \| [110]$	Theory	$2\omega_c, 3\omega_c$	$2\omega_c + \omega_s$
	Exp.	$2\omega_c, 3\omega_c$	$2\omega_c + \omega_s$
$\vec{H} \| [111]$	Theory	$2\omega_c, 2\omega_c + \omega_s$	$3\omega_c$
	Exp.	$2\omega_c, 2\omega_c + \omega_s$	$3\omega_c$

We have made numerical calculations of the peak absorption coefficient α_p for each of the transitions listed in Table VII. Using the expressions of Wallis[31] we find, for a transition $a(n) - f(n')$

$$\alpha_p(\omega) \simeq \frac{4\pi N e^2 \hbar \tau}{ncm^2\omega} \left| \langle f'(n') | \mathcal{H}'_\omega | a'(n) \rangle \right|^2 , \quad (22)$$

where the matrix elements of $\mathcal{H}'_\omega$ are given in Eq. (21), N is the free carrier density, τ the lifetime of the transition, and n the index of refraction. The observed absorption coefficients[5] for the three inversion-asymmetry-induced transitions $2\omega_c$ ($\vec{E} \| \vec{H} \| [001]$) and $2\omega_c + \omega_s$ ($\vec{E} \perp \vec{H} \| [001]$ and $[111]$) which are independent of the impurity and plasma couplings, are consistent with the following three sets of parameters: set a: $C \simeq -3 \times 10^{-9}$ eV cm, $G \simeq -0.21$, $N_2 \simeq -0.61$; set b: $C \simeq -3 \times 10^{-10}$ eV cm, $G \simeq -3$, $N_2 \simeq -1$; set c: $C \simeq 3 \times 10^{-9}$ eV cm, $G \simeq -0.9$, $N_2 \simeq -0.4$, all assuming $N_3 \simeq N_2$ and $G < 0$. For the other three inversion-asymmetry-induced transitions listed in Table VII, which may have contributions from the impurity and plasmon couplings, set a gives approximately the observed absorption coefficients, but the calculated results for set b are too large, and for set c, too small, by up to a factor of about 7. The results for C in sets a and c are about an order of magnitude larger than the result of Pidgeon and Groves,[11] $C \simeq 9.3 \times 10^{-11}$ eV cm. The results for G and N_2 are fairly close to the values estimated in the Appendix ($G \simeq -3.1$ $N_2 \simeq 0.23$) except that in the Appendix we estimate N_2 and G to have opposite signs. Overall, set b is closest to these estimates.

Similarly for the warping-induced transitions in Table VII, we find that from the intensity of the impurity- and plasmon-independent transition $3\omega_c$, $\vec{E} \| \vec{H} \| [111]$ we have $\mu \simeq 2$ using the Pidgeon and Groves value $q \simeq 0.4$ (the results are not sensitive to q), giving, for the other two $3\omega_c$ transitions, peak absorption coefficients about a factor of 5–7 too large. Conversely, the Pidgeon and Groves result $\mu \simeq 0.59$ gives an absorption for the $\vec{E} \| \vec{H} \| [111]$ transition which is about an order of magnitude too small.

In view of the large uncertainty in the experimental results, as well as the approximate nature of our calculations, we regard the above numerical analysis as establishing that the observed warping- and inversion-asymmetry-induced transitions can be accounted for in an approximate way using parameters roughly consistent with their estimated values.

In conclusion, we have obtained the complete 8×8 $\vec{k} \cdot \vec{p}$ Hamiltonian, to first order in magnetic field, for the coupled conduction and valence bands at the Γ point in InSb. We find selection rules for weak cyclotron harmonics in n-type InSb which explain the experimental observations except for one unpredicted absorption line. These weak transitions depend on two new parameters, N_2 and N_3, as well as on other previously defined parameters. Another new parameter N_1 represents a small correction to the conduction-band g factor. It might be possible, once the origin of each experimental cyclotron-harmonic transition is explained and more accurate intensity measurements made, to use a comparison of the experimental and theoretical intensities to determine the six small parameters μ, q, C, G, N_2, and N_3.

ACKNOWLEDGMENTS

We are pleased to acknowledge helpful discussions with G. Favrot, Dr. S. H. Groves and Dr. G. Dresselhaus. We are grateful to Dr. W. Zawadzki for sending us his results prior to publication. This paper is based on a Ph. D. thesis submitted by M. H. Weiler to the Physics Department, Massachusetts Institute of Technology, Cambridge, Mass., 1977. This work was supported by the NSF.

APPENDIX: ESTIMATES OF NEW PARAMETERS

The parameters N_1, N_2, and N_3 are defined by the matrix elements given in Table II or as follows

$$N_1 \equiv -\frac{i}{m} \sum_{\Gamma'_8} \frac{\langle \psi^6_{1/2} | p_x | \Gamma'_8 \rangle \langle \Gamma'_8 | p_y | \psi^6_{1/2} \rangle}{E(\Gamma_6) - E(\Gamma'_8)} ,$$

$$N_2 \equiv \frac{1}{m} \sum_{\Gamma'_8} \frac{\langle \psi^6_{1/2} | p_x | \Gamma'_8 \rangle \langle \Gamma'_8 | p_x | \psi^8_{-3/2} \rangle}{E(\Gamma_8, \Gamma_6) - E(\Gamma'_8)} , \quad (A1)$$

$$N_3 \equiv -\frac{i}{m} \sum_{\Gamma'_8} \frac{\langle \psi^6_{1/2} | p_x | \Gamma'_8 \rangle \langle \Gamma'_8 | p_y | \psi^8_{-3/2} \rangle}{E(\Gamma_8, \Gamma_6) - E(\Gamma'_8)} ,$$

where the summations are over all higher-band Γ'_8 states, and $E(\Gamma_8, \Gamma_6)$ is approximately the average energy of the coupled Γ_6 and Γ_8 conduction and valence bands.

Since these parameters vanish if the spin-orbit coupling is zero, we find estimates for their values to first order in the spin-orbit coupling, starting with the single-group representations. It turns out that, like q, they arise from interactions with higher Γ_4 bands. We denote the conduction band by $\Gamma_1 = (S)$, the valence band by $\Gamma_4 = (X, Y, Z)$ and consider the effects of one higher band $\Gamma'_4 \equiv (X', Y', Z')$. We define, following Ogg,[32]

$$P' \equiv -i(\hbar/m) \langle S | p_x | X' \rangle ,$$
$$Q \equiv -i(\hbar/m) \langle X | p_y | Z' \rangle . \quad (A2)$$

Including spin-orbit coupling the Γ_4' band splits into Γ_8' and Γ_7' bands, with energy separation $E(\Gamma_8') - E(\Gamma_7') \equiv \Delta'$. Performing the spin-orbit transformation on both Γ_4 and Γ_4' and then considering the couplings to second order in P' and Q among the states Γ_6, Γ_7, and Γ_8 gives the $\vec{k}\cdot\vec{p}$ matrices of the forms in Table II proportional to the parameters F, G, and H_1 as well as N_1, N_2, N_3, and q, where H_1 is the parameter defined by Roth *et al.*[14] which contributes to the valence-band parameters γ_1, γ_2, γ_3, and κ. If these parameters arise from only a single Γ_4' band, we find

$$\begin{aligned} F &\simeq -|P'|^2/m[E(\Gamma_8') - \tfrac{1}{3}\Delta' - E(\Gamma_6)], \\ G &\simeq -P'Q^*/m[E(\Gamma_8') - \tfrac{1}{2}\Delta' - E(\Gamma_8, \Gamma_6)], \\ H_1 &\simeq -2|Q|^2/m[E(\Gamma_7') - E(\Gamma_8)], \end{aligned} \tag{A3}$$

with

$$\begin{aligned} N_1 &\simeq F\{\tfrac{1}{3}\Delta'/[E(\Gamma_8') - \tfrac{1}{3}\Delta' - E(\Gamma_6)]\}, \\ N_2 &\simeq -G\{\tfrac{1}{3}\Delta'/\sqrt{2}\,[E(\Gamma_8') - \tfrac{1}{2}\Delta' - E(\Gamma_{8_1}\Gamma_6)]\}, \\ N_3 &\simeq N_2, \\ q &\simeq -H_1\{\tfrac{1}{9}2\Delta'/[E(\Gamma_7') - E(\Gamma_8)]\}. \end{aligned} \tag{A4}$$

The result for q agrees with that of Hensel and Suzuki.[33]

Pidgeon and Groves[11] measured $H_1 \approx -5.6$ and $q = 0.39$ which gives

$$\Delta'/[E(\Gamma_7') - E(\Gamma_8)] \simeq 0.31, \tag{A5}$$

compared to their estimate of 0.21 using $\Delta' \simeq \Delta = 0.8$ eV and $E(\Gamma_8', \Gamma_7') - E(\Gamma_8) \simeq 3.8$ eV. Values which preserve the 0.31 ratio for Eq. (A5) are $\Delta' \simeq 1$ eV and $E(\Gamma_7') - E(\Gamma_8) \simeq 3.2$ eV. Then Eq. (A3) for H_1 gives $|Q|^2/m \simeq 8.9$ eV; we estimate $|P'|^2/m \simeq |P|^2/m \simeq 11$ eV, and obtain for Eqs. (A3) and (A4)

$$\begin{aligned} &F \simeq -3.4, \quad G \simeq -3.1, \quad N_1 \simeq -0.35, \\ &N_2 \simeq 0.23, \quad N_3 \simeq 0.23. \end{aligned} \tag{A6}$$

More recently, Glosser, Fischer, and Seraphin[34] observed electroreflection structure in n-type InSb at approximately 3.1 and 3.5 eV which they attributed to transitions for the Γ_6 to Γ_7' and Γ_8' bands, giving $E(\Gamma_7') - E(\Gamma_6) \simeq 3.1$ eV and $\Delta' \simeq 0.4$ eV. This value of Δ' is about half the Γ_8-Γ_7 splitting Δ and half the value calculated recently by Varea de Alvarez *et al.*,[25] but agrees with a calculation by Bloom and Bergstresser.[36] The above values of Δ' and $E(\Gamma_7') - E(\Gamma_6)$ give a ratio of 0.12 in Eq. (A5), and, given $H_1 \simeq -5.6$, imply $q \simeq 0.15$ rather than 0.39 as found by Pidgeon and Groves.[11]

[1] R. C. Enck, A. L. Saleh, and H. Y. Fan, Phys. Rev. 182, 790 (1969).
[2] E. J. Johnson and D. H. Dickey, Phys. Rev. B 1, 2676 (1970).
[3] R. B. Dennis, R. A. Wood, C. R. Pidgeon, S. D. Smith, and J. W. Smith, J. Phys. C 5, L23 (1972).
[4] M. H. Weiler, R. L. Aggarwal, and B. Lax, Solid State Commun. 14, 299 (1974).
[5] G. Favrot, R. L. Aggarwal, and B. Lax, Solid State Commun. 18, 577 (1976).
[6] B. D. McCombe, S. G. Bishop, and R. Kaplan, Phys. Rev. Lett. 18, 748 (1967).
[7] F. G. Bass and I. B. Levinson, Zh. Eksp. Teor. Fiz. 49, 914 (1965) [Sov. Phys.-JETP 22, 635 (1966)].
[8] R. L. Bell and K. T. Rogers, Phys. Rev. 152, 746 (1966).
[9] M. H. Weiler, R. L. Aggarwal, and B. Lax, Bul. Am. Phys. Soc. 21, 429 (1976); M. H. Weiler, Ph.D. thesis (Massachusetts Institute of Technology, 1977) (unpublished).
[10] W. Zawadzki and J. Wlasak, J. Phys. C 9, L663 (1976).
[11] C. R. Pidgeon and S. H. Groves, Phys. Rev. 186, 824 (1969).
[12] C. R. Pidgeon and R. N. Brown, Phys. Rev. 146, 575 (1966).
[13] J. M. Luttinger, Phys. Rev. 102, 1030 (1956).
[14] L. M. Roth, B. Lax, and S. Zwerdling, Phys. Rev. 114, 90 (1959).
[15] R. R. Goodman, Phys. Rev. 122, 397 (1961).
[16] R. L. Aggarwal, in *Semiconductors and Semimetals*, edited by R. K. Willardson and A. C. Beer (Academic, New York, 1972), Vol. 9, p. 151.
[17] G. F. Koster, J. O. Dimmock, R. G. Wheeler, and H. Statz, *Properties of the Thirty-Two Point Groups* (MIT, Cambridge, 1966).
[18] E. O. Kane, J. Phys. Chem. Solids 1, 249 (1957).
[19] R. N. Dexter, H. J. Zeiger, and B. Lax, Phys. Rev. 104, 637 (1956); H. J. Zeiger, B. Lax, and R. N. Dexter, Phys. Rev. 105, 495 (1957).
[20] G. Dresselhaus, A. F. Kip, and C. Kittel, Phys. Rev. 98, 368 (1955).
[21] S. H. Groves, C. R. Pidgeon, A. W. Ewald, and R. J. Wagner, J. Phys. Chem. Solids 31, 2031 (1970).
[22] M. Reine, Ph.D. thesis (Massachusetts Institute of Technology, 1970) (unpublished); M. Reine, R. L. Aggarwal, and B. Lax, Phys. Rev. B 5, 3033 (1972).
[23] G. Dresselhaus, Phys. Rev. 100, 580 (1955).
[24] It should be pointed out that Eq. (10) of Ref. 12 contains errors in the (5,7) and (7,5) matrix elements: the signs are incorrect, and γ' should read γ''. The sign error was included in the review article by Aggarwal (Ref. 16). Fortunately it has only a small effect on the energies of Landau levels in the conduction and valence bands.
[25] R. Bowers and Y. Yafet, Phys. Rev. 115, 1165 (1959); Y. Yafet, Phys. Rev. 115, 1172 (1959).
[26] K. Lee, B.S. thesis (Massachusetts Institute of Tech-

nology, 1976) (unpublished).
[27]S. J. Miyake, J. Phys. Soc. Jpn. 35, 551 (1973).
[28]B. D. McCombe, R. J. Wagner, S. Teitler, and J. J. Quinn, Phys. Rev. Lett. 28, 37 (1972).
[29]J. Blinowski and J. Mycielski, Phys. Lett. 50A, 88 (1974).
[30]J. J. Quinn, B. D. McCombe, K. L. Ngai, and T. L. Reineke, Phys. Lett. 54A, 161 (1975).
[31]R. F. Wallis, J. Phys. Chem. Solids 4, 101 (1958).
[32]N. R. Ogg, Proc. Phys. Soc. 89, 431 (1966).
[33]J. C. Hensel and K. Suzuki, Phys. Rev. Lett. 22, 838 (1969).
[34]R. Glosser, J. E. Fischer, and B. O. Seraphin, Phys. Rev. B 1, 1607 (1970).
[35]C. Varea de Alvarez, J. P. Walter, R. W. Boyd, and M. L. Cohen, J. Phys. Chem. Solids 34, 337 (1973).
[36]S. Bloom and T. K. Bergstresser, Solid State Commun. 6, 465 (1968).